

# A Preliminary Survey of C-Band RFI in the SMEX04 Area of Operations using WindSat Radiometry

Steven W. Ellingson\*

May 28, 2004

## Contents

<b>1</b>	<b>Introduction</b>	<b>2</b>
<b>2</b>	<b>WindSat</b>	<b>2</b>
<b>3</b>	<b>Analysis</b>	<b>2</b>

---

\*Bradley Dept. of Electrical & Computer Engineering, 340 Whittemore Hall, Virginia Polytechnic Institute & State University, Blacksburg VA 24061 USA. E-mail: [ellingson@vt.edu](mailto:ellingson@vt.edu)

# 1 Introduction

The 2004 Soil Moisture Experiment (“SMEX04”) is scheduled to be conducted in a region southwest of Tucson, AZ and in a nearby area across the border in Mexico [1]. One of the instruments participating in this experiment will be NOAA’s airborne Polar Scanning Radiometer (PSR), augmented with an advanced radio frequency interference (RFI) monitor developed at the Ohio State University. One of the bands targeted for observation using this hybrid system is the “C” Band around 6.8 GHz, which is already known to be severely limited by RFI [2]. For the purposes of planning flight lines, it would be helpful to have advanced knowledge of from where to expect RFI, so that it can be either avoided or observed, depending on the circumstances.

This advance information on RFI distribution can be obtained from an analysis of radiometry from existing systems in Earth orbit, as described in [2]. We are fortunate to have access to radiometry from the WindSat instrument [3], which can be used for this purpose. In this report, a dataset of limited duration (October 2003) is analyzed to determine the spatial distribution of RFI in the 6.8 GHz band in the region of SMEX04.

# 2 WindSat

A detailed description of the WindSat polarimetric microwave radiometer is available in [3]. Here, the details relevant to the analysis in this report are summarized.

WindSat is the primary payload on the U.S. Air Force’s *Coriolis* satellite, which was launched in January 2003 and is now in an 840 km circular sun-synchronous orbit. The 6.8 GHz radiometer has a bandwidth of 125 MHz and integration time of 5 ms, yielding an absolute accuracy of about 0.75 K. WindSat measures brightness temperature in a footprint approximately  $0.5^\circ$  (in latitude and longitude) in diameter as travels over the Earth. For this reason, the “duty cycle” of observation for any given point on the Earth is very low; on the order of twice per day. After ground-based post-processing, radiometry in fully-calibrated vertical (“V”) and horizontal (“H”) polarizations are provided. (“H” refers to the polarization parallel to the ground, whereas “V” refers to the polarization perpendicular to both “H” and the direction of incidence.) Brightness temperatures observed over land in the 6.8 GHz band typically fall in the range 250–330 K. For the purposes of this report, temperatures greater than 330 K are considered RFI, which also corresponds the highest brightness temperature the WindSat radiometer can accurately measure.

The basis of this report was one month of WindSat observations corresponding to the month of October 2003.

# 3 Analysis

The first analysis attempted was to determine the “max hold” brightness temperatures for the SMEX04 area of operations over the observing period. “Max hold” in this case means the maximum brightness temperature in either polarization ever observed at a certain location. This analysis requires the definition of a grid over the surface of the Earth. Each point in the grid defines a pixel for which the brightness temperature statistics are computed. The grid used initially in this report is shown in Figure 1. The grid spacing is set equal to four times the mean spacing of the swath data obtained from WindSat. This grid spacing is approximately one-half of a beamwidth, so there is significant spatial overlap in both the WindSat data as well as the observations presented here.

Figure 2 shows the probability distribution function (PDF) of the number of observations per grid point. An “observation” is defined as follows: For each measurement from WindSat, the grid point nearest the center of the beam is determined, and then this grid point (and no other) is then declared to have been observed. Note that each grid point is observed at least 46 times over the one month period, with a typical value being closer to twice a day over that period.

Using this approach, Figure 3 shows the max-hold brightness temperature, displayed as a flat-shaded contour plot. Note that some caution is required in interpreting this plot since the graphing routine is essentially interpolating between the points shown in Figure 1 to obtain the temperatures

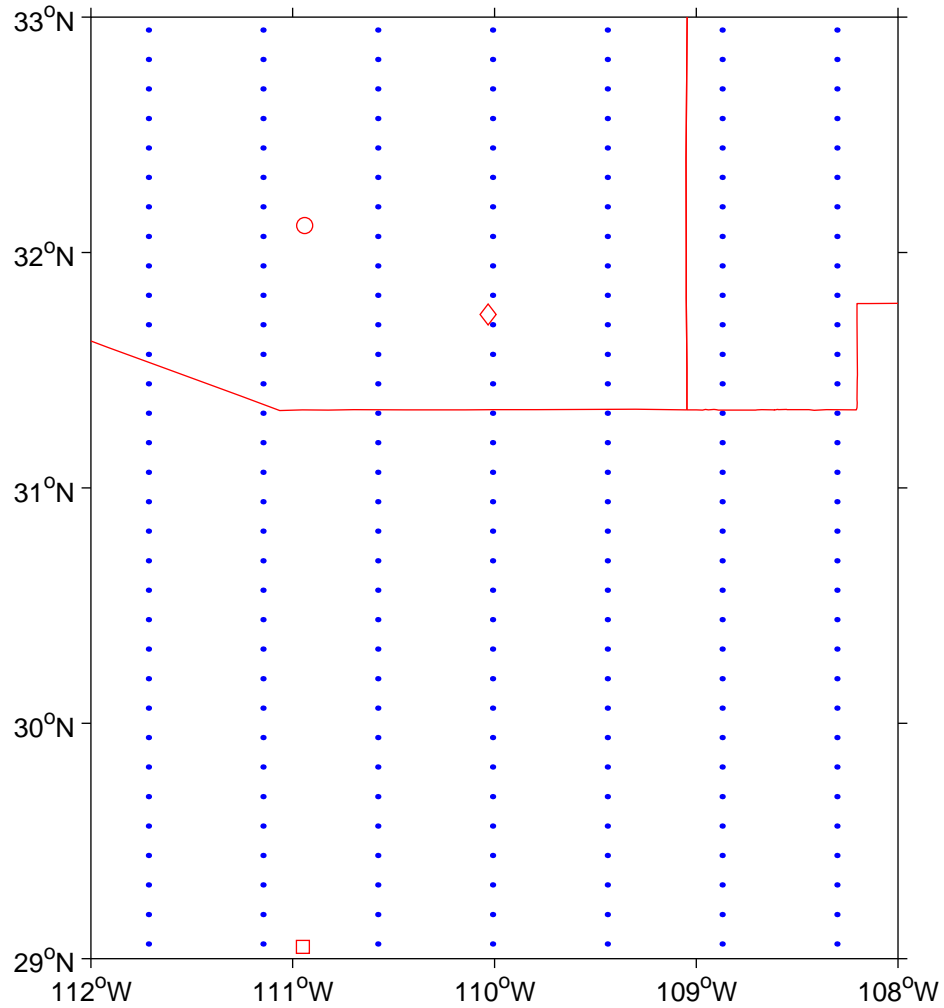


Figure 1: Grid used to compute max-hold and average brightness temperature distributions. The red lines denote the common borders of Arizona, New Mexico, and Mexico. The circle, diamond, and square correspond to Tucson (AZ) International Airport, the Walnut Gulch Watershed benchmark, and Hermosillo, Mexico, respectively. The SMEX04 area of operations includes two non-contiguous areas, one approximately centered on Walnut Gulch, and the other just south of the border in Mexico.

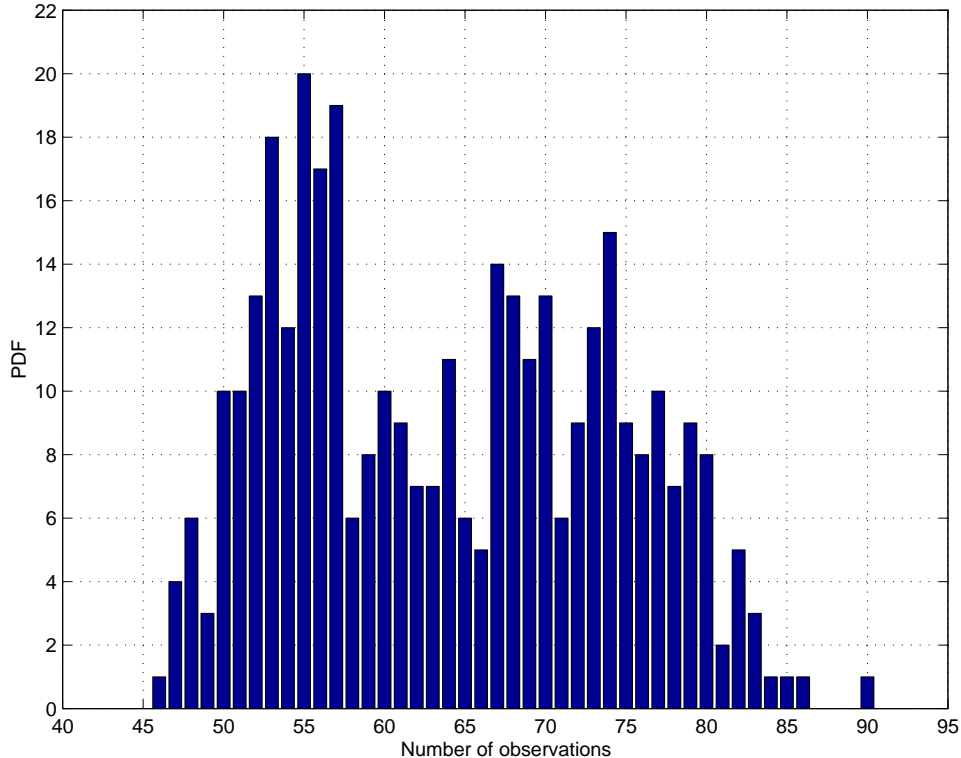


Figure 2: Distribution of the number of observations per grid point.

at all other points. Nevertheless, we see that a large area centered on Tucson, AZ exhibits brightness temperatures in excess of 330 K, strongly suggesting the presence of RFI, whereas other locations exhibit no RFI.

Figures 4 and 5 show the *mean* brightness temperatures over all observations in the vertical and horizontal polarizations respectively. In both cases, the region around Tucson is still clearly visible as a source of RFI, and the vertical polarization appears to be significantly stronger than the horizontal polarization. This appears to be independent of the fact that the geophysical brightness temperature signal is also stronger in the vertical polarization than the horizontal polarization, as can be seen in the PDF shown in Figure 6.

To better resolve the spatial and temporal statistics of the RFI, a different analysis was attempted using grid similar to the one showed in Figure 1 but four times finer; i.e. spatial sampling approximately equal to that of the original data. Of course, the number of observations per grid point is greatly reduced in this approach, because there is a higher density of grid points available to “accept” observations. As shown in Figures 7 and 8, the number of observations per grid point is reduced to an average of about 5 (i.e., about once a week) and a few points are never observed. The latter are relatively few and are plotted in Figure 9 to show that they are unlikely to significantly bias the results.

Using the fine grid, Figure 10 shows all grid points experiencing at least one observation of RFI (i.e., at least one recorded brightness temperature greater than 330 K in either polarization). We see that these are primarily concentrated around Tucson, with a second cluster appearing to the directly to the east and slightly north of the AZ SMEX04 area of operations. Although none of the interference discussed in this report has been attributed to a source, this second cluster is particularly intriguing since it does not seem to be associated with population density. An intriguing possibility is that it is multipath scattering from the mountainous region to the east and north of Tucson, as shown in Figure 11.

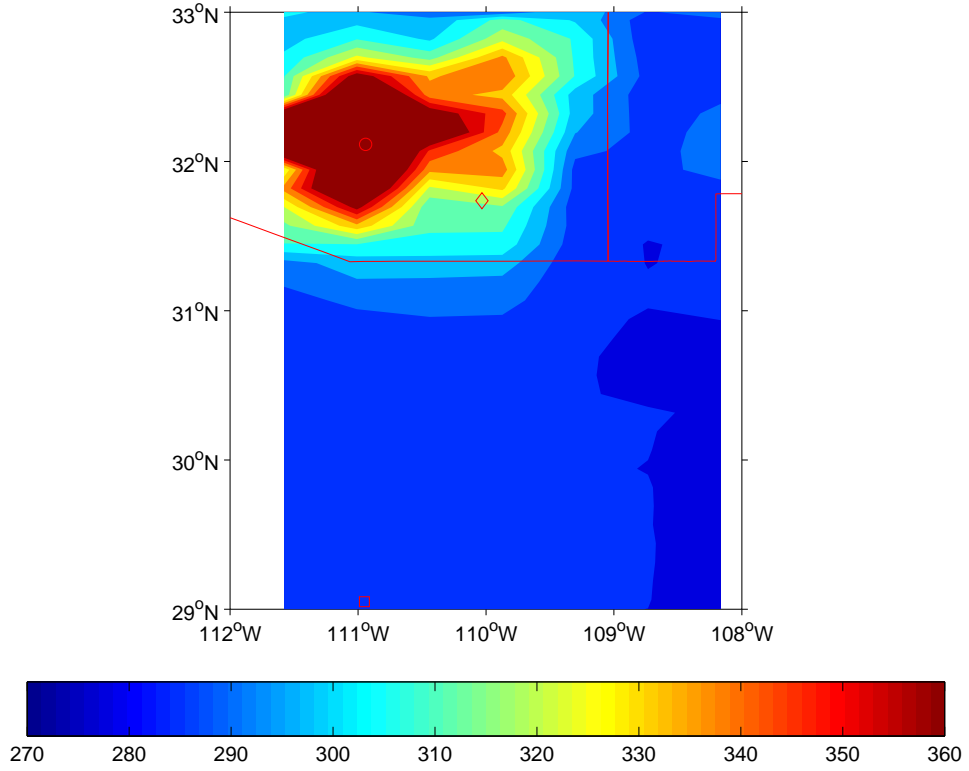


Figure 3: "Max Hold" Brightness Temperature.

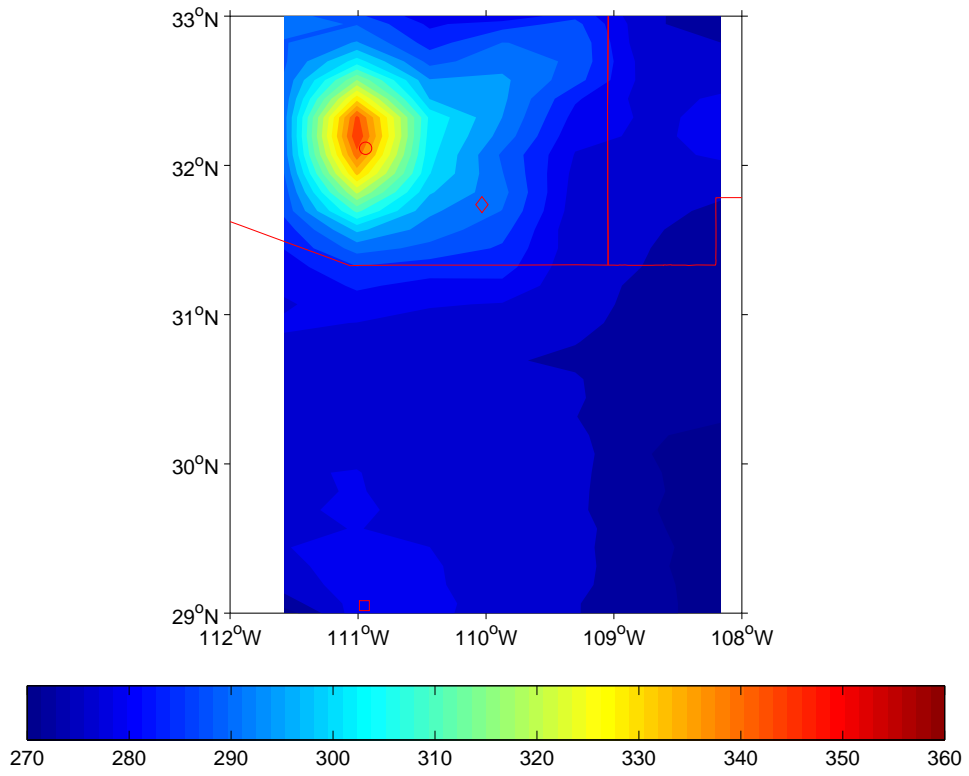


Figure 4: Mean Brightness Temperature, Vertical Polarization.

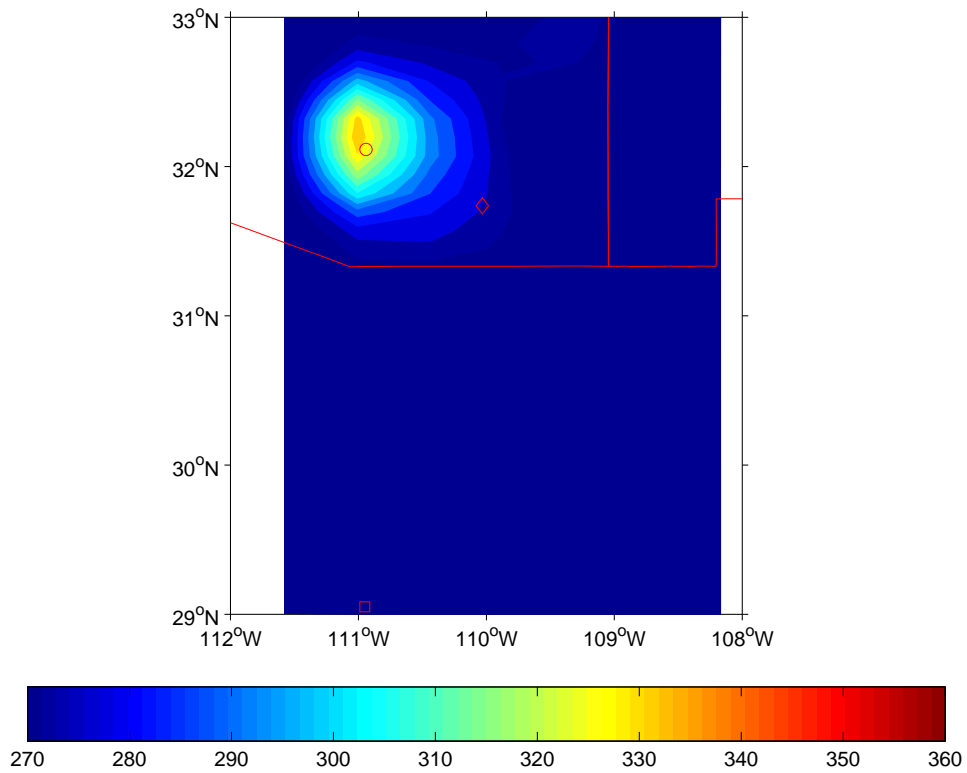


Figure 5: Mean Brightness Temperature, Horizontal Polarization.

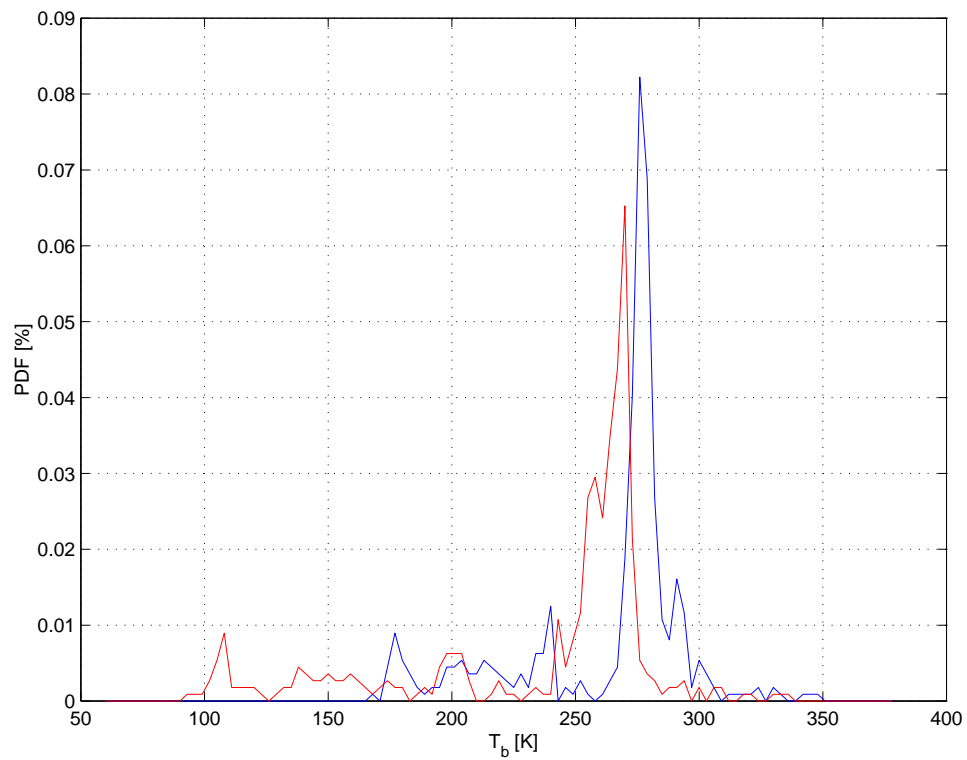


Figure 6: PDF of mean brightness temperature. *Blue*: Vertical polarization, *Red*: Horizontal polarization.

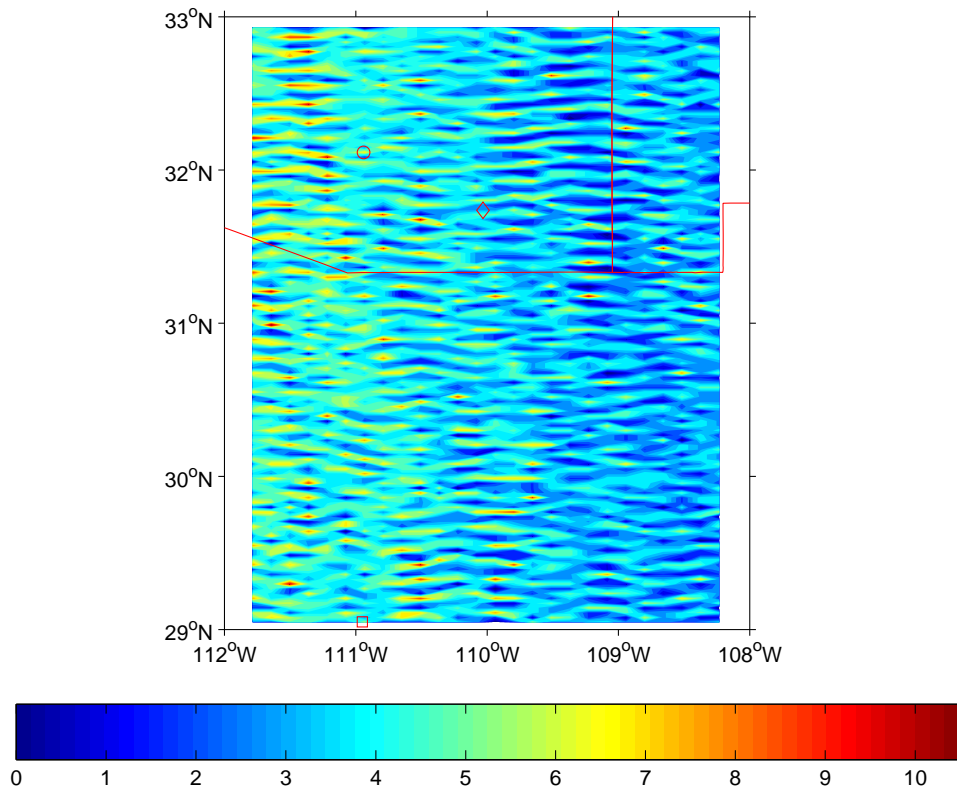


Figure 7: Number of observations per grid point using the second (fine) grid.

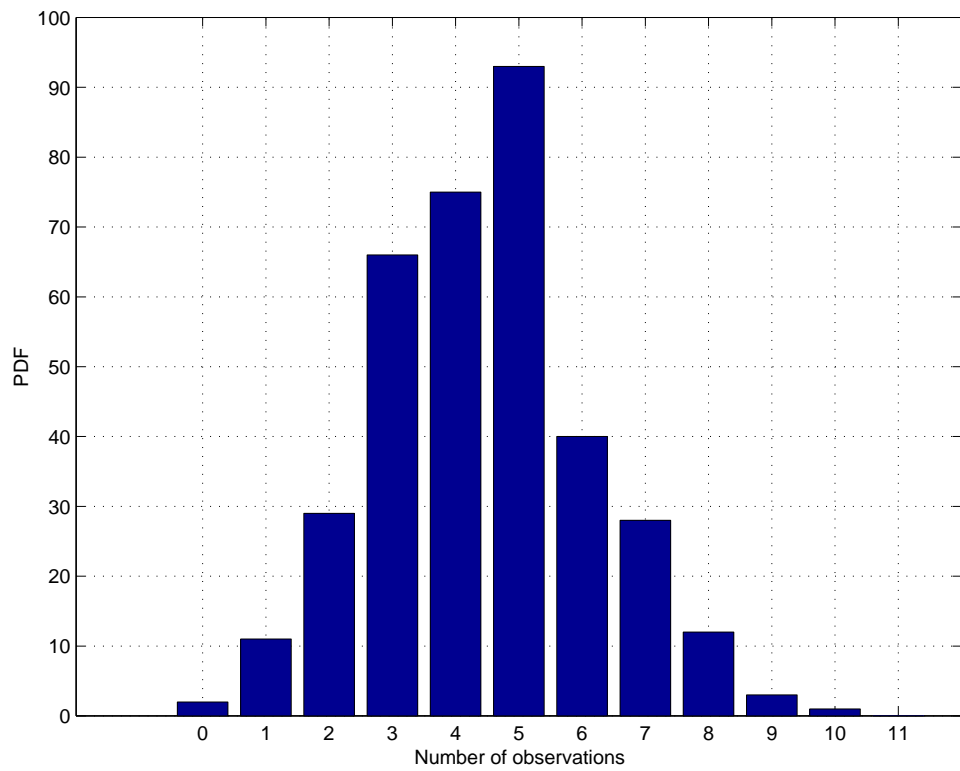


Figure 8: PDF of the number of observations per grid point using the second (fine) grid.

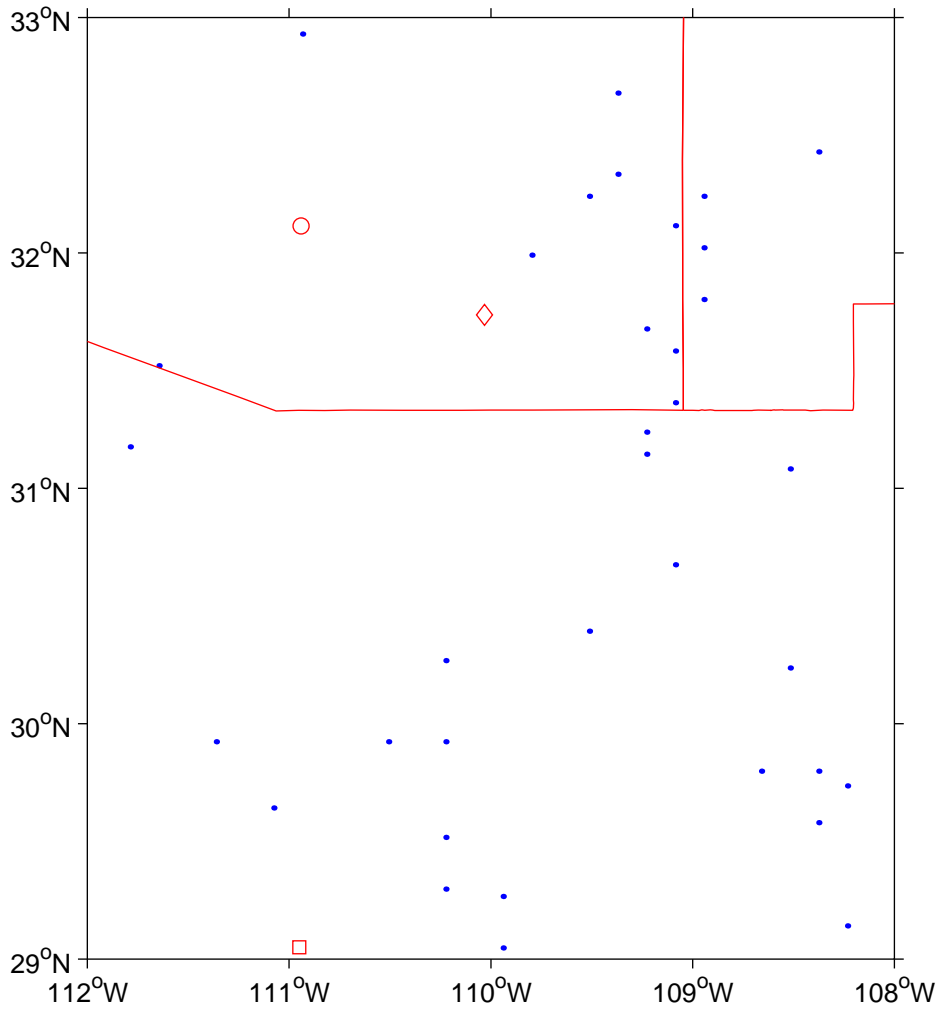


Figure 9: Locations of unobserved grid points using the second (fine) grid.

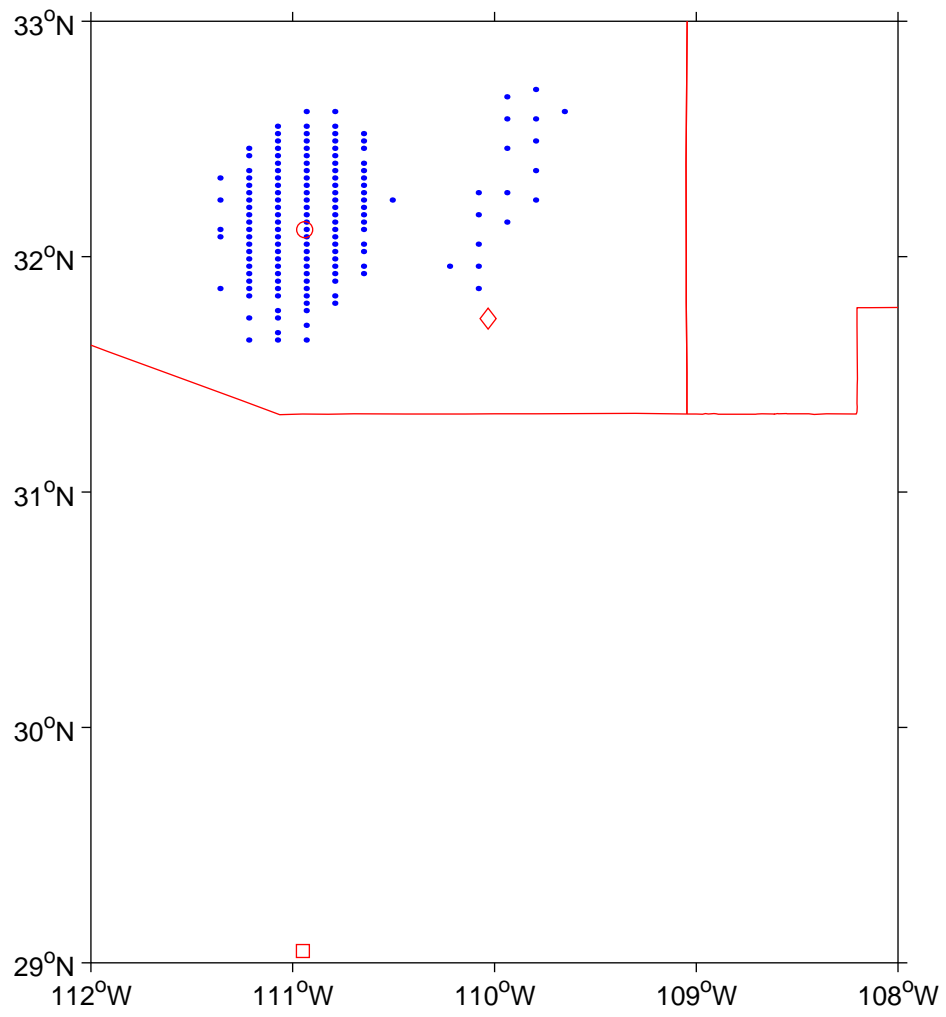


Figure 10: Grid points experiencing at least one observation of RFI.

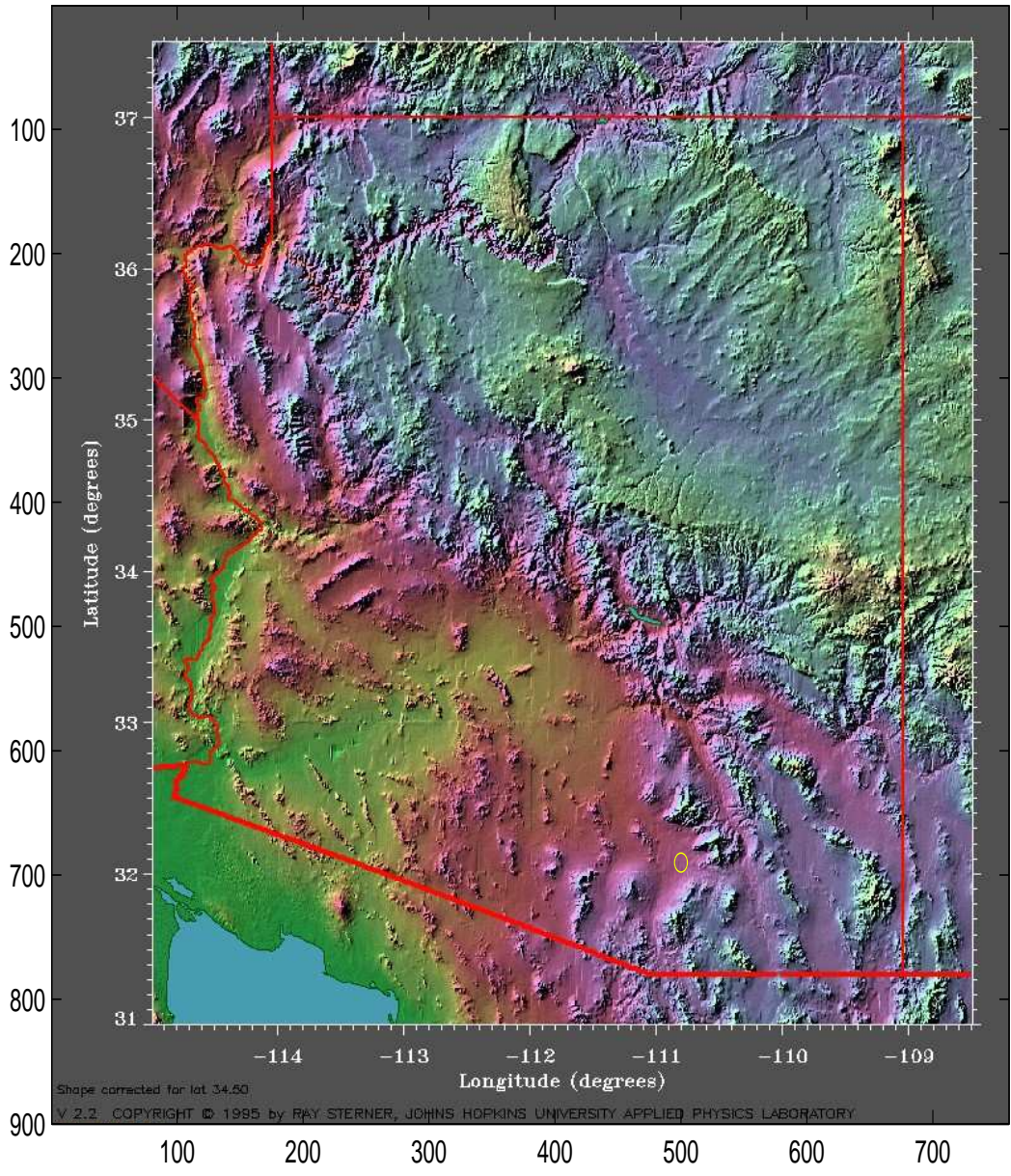


Figure 11: Map showing terrain topology of Arizona. The approximate position of Tucson is indicated by a yellow circle.

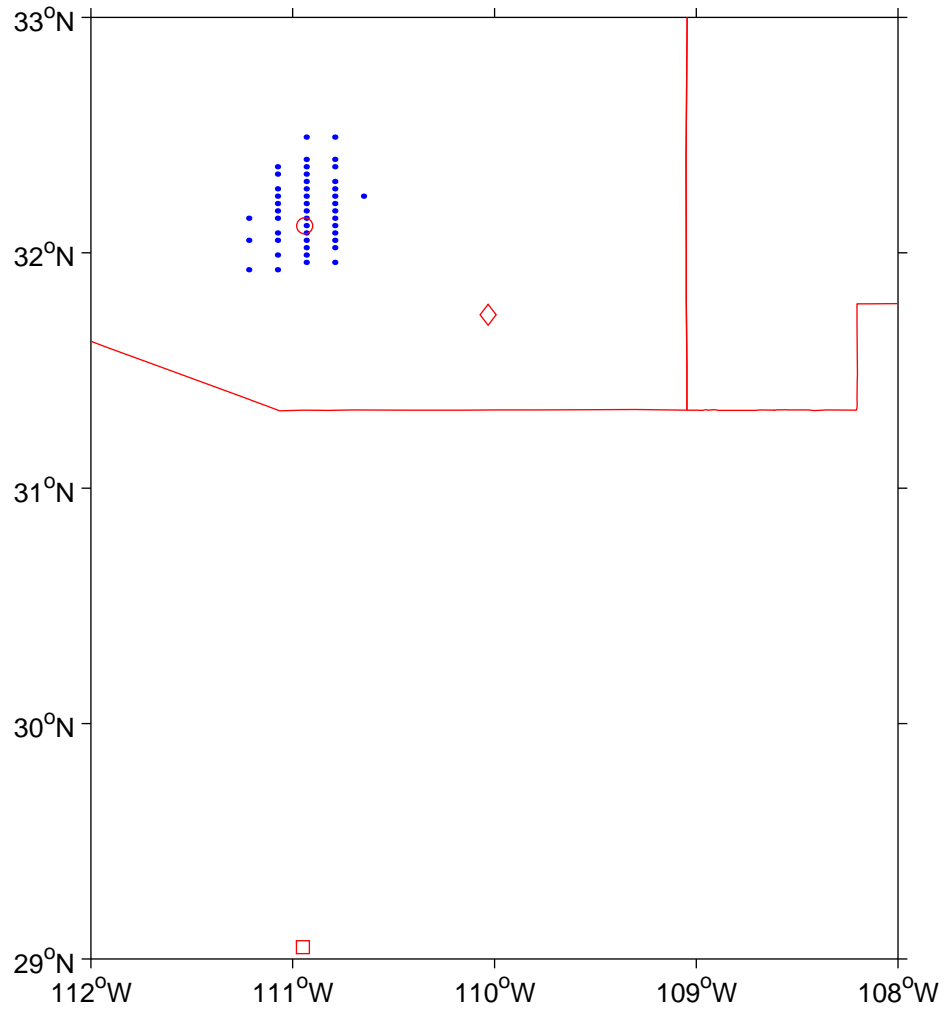


Figure 12: Grid points exhibiting RFI during *every* observation.

Finally, Figure 12 shows all grid points for which RFI was observed during *every* observation. Note that the interference associated with Tucson remains, and the second cluster vanishes. Thus, the mechanism associated with this second cluster must be intermittent or perhaps periodic.

## References

- [1] “Soil Moisture Experiment 2004 (SMEX04) and the North American Monsoon Experiment (NAME): Preliminary Experiment Plan”, November 2003.
- [2] L. Li *et al.*, “A Preliminary Survey of Radio-Frequency Interference over the U.S. in Aqua AMSR-E Data,” *IEEE Trans. Geoscience & Remote Sensing*, **42**, 380, 2004.
- [3] P.W. Geiser *et al.*, “The WindSat Space Borne Polarimetric Microwave Radiometer: Sensor Description and Early Orbit Performance”, Submitted to *IEEE Trans. Geoscience & Remote Sensing*, February 10, 2004.